heteroatoms. The highest level calculations of Pople et al.[20] corroborate this by showing that $H_5O_2^+$, $H_3F_2^+$, and $H_3Cl_2^+$ have single minimum potential energy wells with the proton sysmmetrically bound by the two monomer bases. Further, even through $N_2H_7^+$ is predicted to have a double minimum potential energy well, the central barrier is only 1.0 kcal mol^{-1}, indicating that the zero-point energy of the vibrations about the hydrogen bond will readily carry the proton over the maximum.

Conclusions

Experimental evidence has been presented to show that the proton bound dimer of methyl fluoride, $(CH_3F)_2H^+$ (and by implication that of $(HF)_2H^+$), exhibits a very strong hydrogen bond of 32 ± 2 kcal mol^{-1}. Such strong hydrogen bonding involving monomers of very low base strength offers strong support for Allen's contention that hydrogen bonding will be greatest for species involving electronegative atoms. Available experimental data and ab initio calculation show a strong correlation between electronegativity and hydrogen bond strength in symmetric proton bound dimers. Work is currently in progress on binding energies of proton bound dimers of a variety of sulfur, phosphorus, chlorine, and bromine bases to determine effects of substitution on the heteroatom on hydrogen bond strength.

Acknowledgment. Financial support of this work by N.S.E.R.C. (Canada) grants to T. B. McMahon and P. Kebarle is gratefully acknowledge. T. B. McMahon thanks the Department of Chemisty, University of Alberta, for hospitality and financial support during a sabbatical leave while these experiments were carried out.

Registry No. $CH_3F{\cdot}H^+$, 59122-96-2; CH_3F, 593-53-3; $SO_2{\cdot}H^+$, 103905-48-2; SO_2, 7446-09-5; H^+, 12408-02-5.

Penning Ionization Electron Spectroscopy of Monohalogenobenzenes: C_6H_5F, C_6H_5Cl, C_6H_5Br, and C_6H_5I

S. Fujisawa,[†] K. Ohno,[‡] S. Masuda,[‡] and Y. Harada*[‡]

Contribution from the Department of Chemistry, Faculty of Science, Toho University, Funabashi, Chiba 274, Japan, and Department of Chemistry, College of Arts and Sciences, The University of Tokyo, Komba, Meguro, Tokyo 153, Japan. *Received January 2, 1986*

Abstract: He*(2^{3}S) Penning ionization electron spectra (PIES) and He I ultraviolet photoelectron spectra (UPS) were measured to study the electronic structures and reactivities of monohalogenobenzenes. On the basis of the feature of PIES which provides direct information on the spatial distribution of individual molecular orbitals, all the bands in the UPS were assigned. Since Penning ionization can be interpreted as an electrophilic reaction in which a metastable atom extracts an electron from an occupied orbital of a molecule, the relative reactivity of the orbital upon electrophilic attack can be studied from the relative intensity of the bands in PIES. It was found that the reactivity of the n and π orbitals of monohalogenobenzenes depends on the electronic factor due to the size of the halogen p orbitals and the conjugation between the benzene ring and the halogene atoms, and also on the steric factor due to the benzene ring shielding some orbitals from the impact of metastable atoms.

Penning ionization electron spectroscopy is based on the energy analysis of electrons released in the ionization of atoms or molecules M by impact of metastable atoms A*:[1]

$$M + A^* \rightarrow M^+ + A + e^- \quad (1)$$

In this process an electron in an orbital of M transfers into the vacant orbital of A* and its excited electron is ejected.[2] Since the probability of the electron transfer is essentially determined by spatial overlap of the relevant orbital of M and the vacant orbital of A*, an outer orbital exposed outside the repulsive (van der Waals) surface of the molecule gives a stronger band in the Penning ionization electron spectrum (PIES) than does an inner orbital localized inside the surface.[3] Thus, the relative band intensity of the spectrum depends on the spatial electron distribution of individual molecular orbitals. Using this feature of PIES, we have successfully assigned the bands in ultraviolet photoelectron spectra (UPS) of various organic molecules.[3-11] Furthermore, the studies of the electron distribution of individual orbitals exposed outside solid surfaces have enabled us to probe the geometrical orientation and electronic state of molecules at the outermost surface layer.[12,13]

From a chemical point of view, Penning ionization process 1 is regarded as an electrophilic reaction of an excited atom A* with a molecule M; the reagent A* attacks an orbital of M and extracts an electron into the vacant orbital of A* yielding an ionic state of M^+.[3,10] In this respect, the intensity of a band in PIES is connected with the reactivity of the corresponding orbital upon

[†] Toho University.
[‡] The University of Tokyo.

(1) Čermák, V. *J. Chem. Phys.* **1966**, *44*, 3781-3786.
(2) Hotop, H.; Niehaus, A. *Z. Phys.* **1969**, *228*, 68-88.
(3) Ohno, K.; Mutoh, H.; Harada, Y. *J. Am. Chem. Soc.* **1983**, *105*, 4555-4561.
(4) Munakata, T.; Kuchitsu, K.; Harada, Y. *Chem. Phys. Lett.* **1979**, *64*, 409-412. Munakata, T.; Kuchitsu, K.; Harada, Y. J. *Electron Spectrosc. Relat. Phenom.* **1980**, *20*, 235-244. Munakata, T.; Ohno, K.; Harada, Y.; Kuchitsu, K. *Chem. Phys. Lett.* **1981**, *83*, 243-245.
(5) Munakata, T.; Harada, Y.; Ohno, K.; Kuchitsu, K. *Chem. Phys. Lett.* **1981**, *84*, 6-8.
(6) Ohno, K.; Fujisawa, S.; Mutoh, H.; Harada, Y. *J. Phys. Chem.* **1982**, *86*, 440-441.
(7) Veszprēmi, T.; Harada, Y.; Ohno, K.; Mutoh, H. *J. Organomet. Chem.* **1983**, *244*, 115-118; **1983**, *252*, 121-125; **1984**, *266*, 9-16. Veszprēmi, T.; Bihātsi, L.; Harada, Y.; Ohno, K.; Mutoh, H. *Ibid.* **1985**, *280*, 39-43.
(8) Harada, Y.; Ohno, K.; Mutoh, H. *J. Chem. Phys.* **1983**, *79*, 3251-3255.
(9) Ohno, K.; Imai, K.; Matsumoto, S.; Harada, Y. *J. Phys. Chem.* **1983**, *87*, 4346-4348.
(10) Ohno, K.; Matsumoto, S.; Imai, K.; Harada, Y. *J. Phys. Chem.* **1984**, *88*, 206-209.
(11) Ohno, K.; Matsumoto, S.; Harada, Y. *J. Chem. Phys.* **1984**, *81*, 4447-4454.
(12) Munakata, T.; Ohno, K.; Harada, Y. *J. Chem. Phys.* **1980**, *72*, 2880-2881. Kubota, H.; Munakata, T.; Hirooka, T.; Kuchitsu, K.; Harada, Y. *Chem. Phys. Lett.* **1980**, *74*, 409-412. Ohno, K.; Mutoh, H.; Harada, Y. *Surf. Sci.* **1982**, *115*, L128-L132. Kubota, H.; Munakata, T.; Hirooka, T.; Kondow, T.; Kuchitsu, K.; Ohno, K.; Harada, Y. *Chem. Phys.* **1984**, *87*, 399-403. Harada, Y.; Ozaki, H.; Ohno, K. *Phys. Rev. Lett.* **1984**, *52*, 2269-2272. Harada, Y.; Ozaki, H.; Ohno, K.; Kajiwara, T. *Surf. Sci.* **1984**, *147*, 356-360.

0002-7863/86/1508-6505$01.50/0

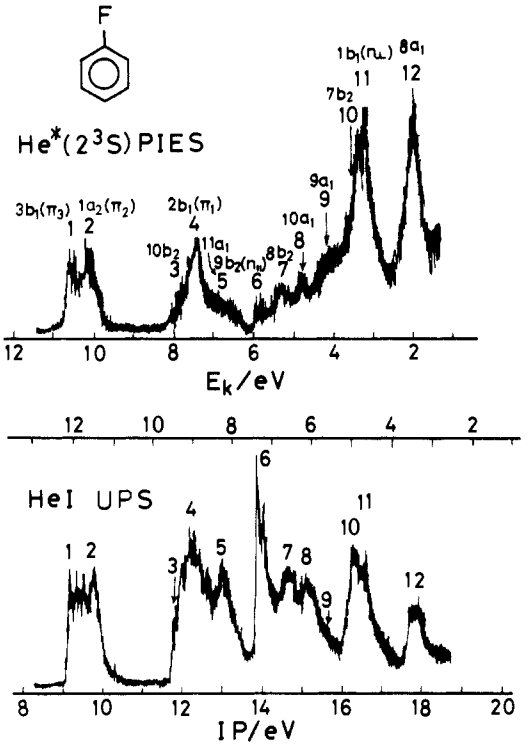

Figure 1. He*(2³S) PIES and He I UPS of fluorobenzene.

electrophilic attack by metastable atoms. Thus, an orbital exposed to the outside of the molecular surface is more reactive than an orbital localized inside the surface. Furthermore, with the introduction of a bulky group, some molecular orbitals can be protected from the impact of metastables and become less reactive. Such a steric shielding effect has been observed in the PIES of organometallic complexes[5,8] and also of some substituted anilines[6] and nitriles.[10]

In this paper, firstly, we intend to establish the assignments of the bands in the UPS of monohalogenobenzenes, C_6H_5F, C_6H_5Cl, C_6H_5Br, and C_6H_5I, on the basis of the characteristics of PIES mentioned above. MO calculations were also carried out for C_6H_5F and C_6H_5Cl. Although extensive studies have been made for the UPS of monohalogenobenzenes,[14-21] the assignments of some bands are still ambiguous. Secondly, we aim to study the relative PIES activity of the π and n orbitals of monohalogenobenzenes. Such a study is of considerable chemical significance because it provides insight into the role of the π and n orbitals in electrophilic reactions of the compounds.

Experimental Section

He*(2³S) PIES and He I UPS were measured using the electron spectrometer described elsewhere.[8] Thermal He atoms were excited to the metastable states (2¹S 20.62 eV, and 2³S 19.82 eV) by impact of 60-eV electrons. A water-cooled helium discharge lamp was used to quench the 2¹S metastable atoms, and pure He*(2³S) beams were ob-

Table I. Observed and Calculated Ionization Potentials of Fluorobenzene

	IP_{obsd}/eV	IP_{calcd}/eV	MO character[a]
1	9.20	9.27	$3b_1$, π_3
2	9.83	9.55	$1a_2$, π_2
3	11.8	13.66	$10b_2$
4	12.28	13.81	$2b_1$, π_1
5	13.06	14.35	$11a_1$
6	13.89	16.09	$9b_2$, $n_\parallel$
7	14.70	16.44	$8b_2$
8	15.11	17.02	$10a_1$
9	15.7	18.59	$9a_1$
10	16.30	18.88	$7b_2$
11	16.6	18.52	$1b_1$, $n_\perp$
12	17.82	20.09	$8a_1$

[a] The symbol $n_\parallel$ or $n_\perp$ indicates the orbital predominantly due to the fluorine 2p orbital distributed parallel or perpendicular to the benzene ring.

Table II. Observed and Calculated Ionization Potentials of Chlorobenzene

	IP_{obsd}/eV	IP_{calcd}/eV	MO character[a]
1	9.08	9.10	$4b_1$, π_3
2	9.70	9.50	$1a_2$, π_2
3	11.33	12.22	$9b_2$, $n_\parallel$
4	11.66	12.65	$3b_1$, $n_\perp$
5	12.25	13.69	$15a_1$
6	13.0	13.92	$8b_2$
7	13.17	14.79	$2b_1$, π_1
8	14.27	15.88	$14a_1$
9	14.60	16.38	$7b_2$
10	15.31	17.63	$6b_2$
11	15.7	17.50	$13a_1$
12	16.91	19.34	$12a_1$

[a] The symbol $n_\parallel$ or $n_\perp$ indicates the orbital predominantly due to the chlorine 3p orbital distributed parallel or perpendicular to the benzene ring.

Table III. Observed Ionization Potentials of Bromobenzene

	IP_{obsd}/eV	MO character[a]
1	9.00	b_1, π_3
2	9.64	a_2, π_2
3	10.65	b_2, $n_\parallel$
4	11.20	b_1, $n_\perp$
5	12.00	a_1
6	12.70	b_2
7	12.9	b_1, π_1
8	14.10	a_1
9	14.50	b_2
10	15.17	a_1
11	15.70	b_2
12	16.81	a_1

[a] The symbol $n_\parallel$ or $n_\perp$ indicates the orbital predominantly due to the bromine 4p orbital distributed parallel or pependicular to the benzene ring.

Table IV. Observed Ionization Potentials of Iodobenzene

	IP_{obsd}/eV	MO character[a]
1	8.79	b_1, π_3
2	9.53	a_2, π_2
3	9.77	b_2, $n_\parallel$
4	10.58	b_1, $n_\perp$
5	11.62	a_1
6	12.39	b_2
7	12.7	b_1, π_1
8	13.62	a_1
9	14.30	b_2
10	15.03	a_1
11	15.5	b_2
12	16.70	a_1

[a] The symbol $n_\parallel$ or $n_\perp$ indicates the orbital predominantly due to the iodine 5p orbital distributed parallel or perpendicular to the benzene ring.

(13) Harada, Y. *Surf. Sci.* **1985**, *158*, 455-472.
(14) Baker, A. D.; May, D. P.; Turner, D. W. *J. Chem. Soc. B* **1968**, 22-34. Murrell, J. N.; Suffolk, R. J. *J. Electron Spectrosc. Relat. Phenom.* **1972/73**, *1*, 471-480. Debies, T. P.; Rabalais, J. W. *Ibid.* **1972/73**, *1*, 355-370. Duke, C. B.; Yip, K. L.; Ceaser, G. P. *J. Chem. Phys.* **1977**, *66*, 256-268.
(15) Cvitaš, T.; Klasinc, L. *Croat. Chem. Acta* **1977**, *50*, 291-297.
(16) Cvitaš, T.; Güsten, H.; Klasinc, L. *J. Chem. Soc., Perkin Trans. 2* **1977**, 962-965.
(17) Sell, J. A.; Kuppermann, A. *Chem. Phys.* **1978**, *33*, 367-378.
(18) Potts, A. W.; Lyus, M. L.; Lee, E. P. F.; Fattahallah, G. H. *J. Chem. Soc., Faraday Trans. 2* **1980**, *76*, 556-570.
(19) Ruščič, B.; Klasnic, L.; Wolf, A.; Knop, J. V. *J. Phys. Chem.* **1981**, *85*, 1486-1489.
(20) Kimura, K.; Katsumata, S.; Achiba, Y.; Yamazaki, T.; Iwata, S. *Handbook of He I Photoelectron Spectra of Fundamental Organic Molecules*; Japan Scientific Societies Press: Tokyo, 1981, and refrences therein.
(21) Niessen, W.; Åsbrink, L.; Bieri, G. *J. Electron Spectrosc. Relat. Phenom.* **1982**, *26*, 173-201, and references therein.

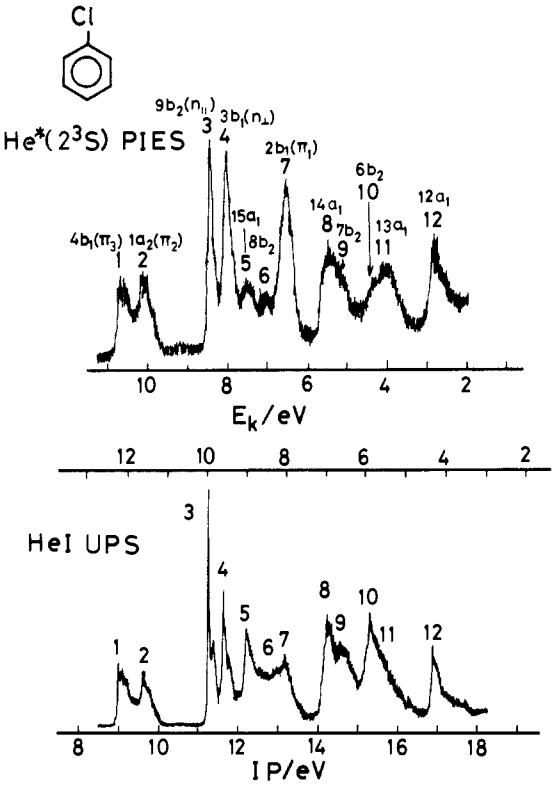

Figure 2. He*(2³S) PIES and He I UPS of chlorobenzene.

tained. The He I resonance line (21.22 eV) for UPS was produced by dc discharge in pure He gas. Electron spectra were obtained at an ejection angle of 90° with respect to the metastable atom beam or the photon beam. The relative band intensity of the spectra was calibrated using the transmission efficiency curve of the spectrometer.[3]

Calculations. The molecular orbitals of fluorobenzene and chlorobenzene were calculated by the ab initio method with a 4-31G basis set[22] using the library program GSCF2 at the Computer Center, The University of Tokyo.[23] The coordinate axes for the molecules are shown in Figure 10.

Results

Figures 1–4 show the He*(2³S) PIES and He I UPS of C_6H_5F, C_6H_5Cl, C_6H_5Br, and C_6H_5I. The electron energy scales for the PIES are shifted relative to those for the UPS by the difference in the excitation energies, (21.22 − 19.82) eV = 1.40 eV. Tables I–IV list the vertical ionization potentials (IP's) of monohalogenobenzenes obtained from the UPS (Figures 1–4) together with their assignments to respective MO's. For C_6H_5F and C_6H_5Cl the calculated IP's via Koopmans' theorem[24] are also included in the tables.

Figures 5 and 6 show the shapes of the occupied molecular orbitals of C_6H_5F and C_6H_5Cl listed in Tables I and II. In the figures the orbital coefficients are shown by circles or couples of ellipses whose area are proportional to the square of the coefficients. The solid and broken circles indicate the s orbital and the out-of-plane p orbital, respectively, while the couple of ellipses show the in-plane p orbital. The thick and thin curves indicate the lobes with positive and negative signs.

Discussion

Assignments of UPS Bands. (1) Fluorobenzene. As was described in the introductory section, we can assign bands in UPS on the basis of the relative intensity of the corresponding PIES bands. In the 11–6-eV region of the PIES in Figure 1, bands 1, 2, and 4 are enhanced relative to the other bands. Since the π

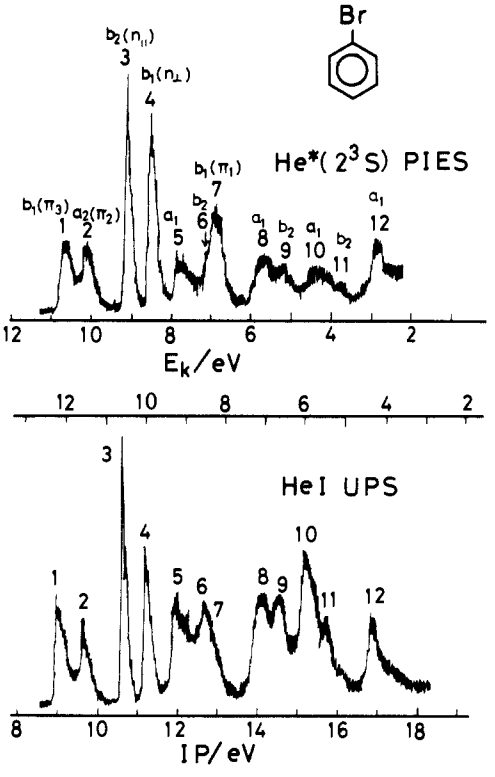

Figure 3. He*(2³S) PIES and He I UPS of bromobenzene.

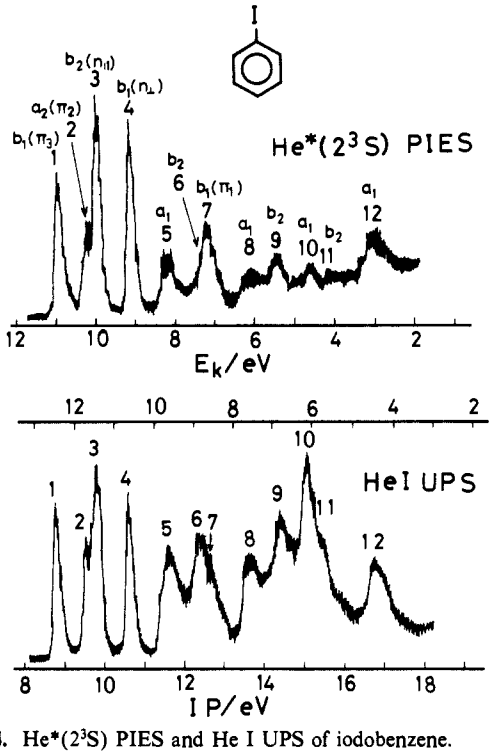

Figure 4. He*(2³S) PIES and He I UPS of iodobenzene.

bands due to the benzene ring appear in this region[25,26] and should be enhanced in the PIES owing to the character of the π orbitals widely distributed outside the molecular surface, we can assign bands 1, 2, and 4 to the $3b_1(\pi_3)$, $1a_2(\pi_2)$, and $2b_1(\pi_1)$ orbitals. The $3b_1$ and $1a_2$ orbitals are derived from the splitting of the $1e_{1g}$ orbitals of benzene, while the $2b_1$ orbital is related to the benzene $1a_{2u}$ orbital. The enhancement of π bands in PIES has been

(22) Ditchfield, R.; Hehre, W. J.; Pople, J. A. *J. Chem. Phys.* **1971**, *54*, 724–728.
(23) Kosugi, N. Program GSCF2, Program Library, The Computer Center, The University of Tokyo, 1981.
(24) Koopmans, T. *Physica (Utrecht)* **1933**, *1*, 104–113.
(25) Turner, D. W.; Baker, C.; Baker, A. D.; Brundle, C. R. *Molecular Photoelectron Spectroscopy*; Wiley-Interscience: London, 1970.
(26) Åsbrink, L.; Edquist, O.; Lindholm, E.; Selin, L. E. *Chem. Phys. Lett.* **1970**, *5*, 192–194.

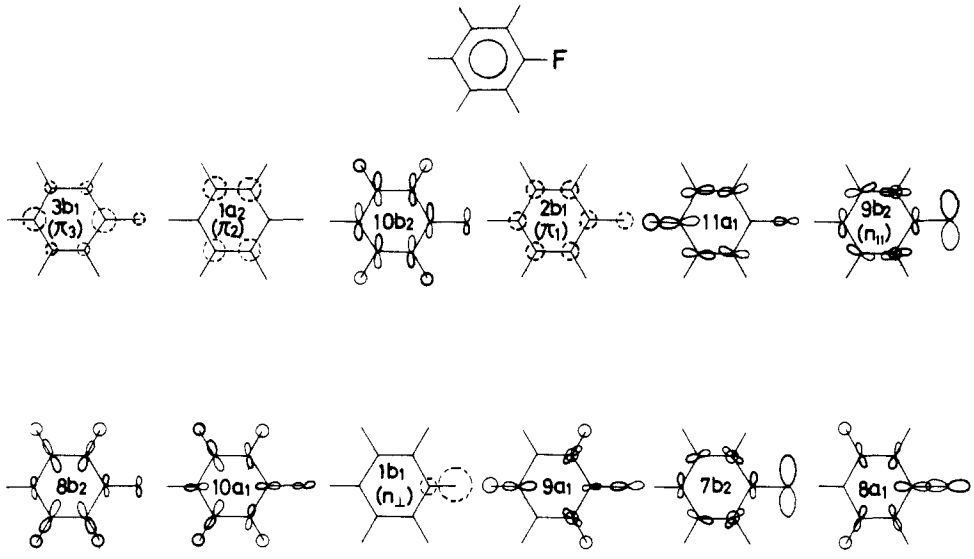

Figure 5. The shapes of the occupied molecular orbitals of fluorobenzene listed in Table I.

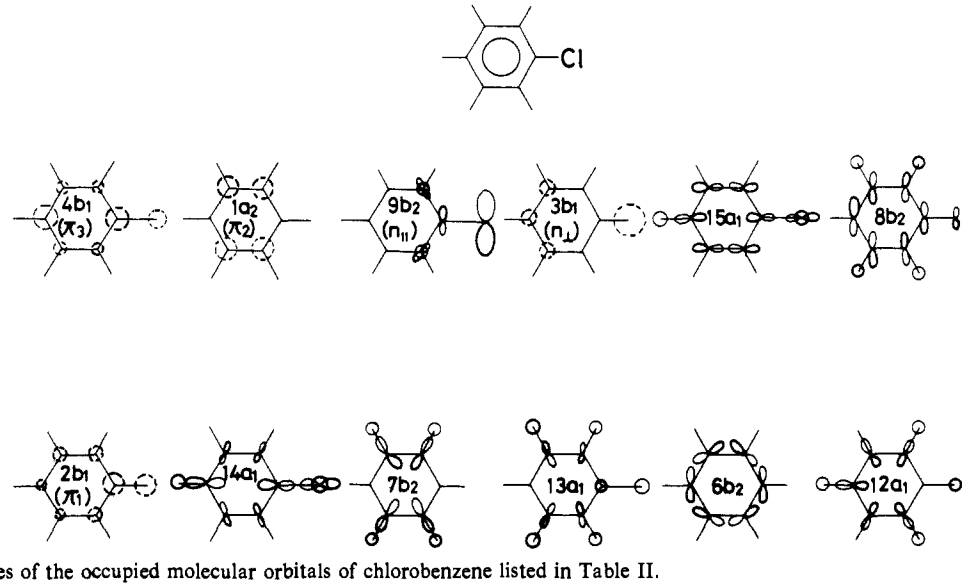

Figure 6. The shapes of the occupied molecular orbitals of chlorobenzene listed in Table II.

observed in many conjugated molecules.[3,4,11]

In Figure 1 the sharpness of band 6 in the UPS suggests that this band is due to a nonbonding orbital of the fluorine atom. From a comparison between the calculated and observed IP's in Table I we can assign band 6 to the $9b_2(n_{\parallel})$ orbital, which is predominantly due to the fluorine $2p_x$ orbital distributed parallel to the benzene ring (cf. Figure 5). As can be seen in Figure 1, the corresponding band 6 in the PIES is weak. This is explained from a steric shielding effect of the benzene ring. As described before, such a shielding effect of bulky groups has been found in various compounds.[5,6,8,10]

The assignments of bands 1 to 6 in Table I are in agreement with those by Kimura et al.[20] except that they related the peak at IP 12.3 eV in the UPS to both the $10b_2$ and $2b_1(\pi_1)$ orbitals. In view of the shape of the PIES, we assigned the shoulder at IP 11.8 eV in the UPS to the $10b_2$ orbital.

In Figure 1 bands 11 and 12 are much stronger in comparison with the other bands in the 6–1-eV region of the PIES. We assigned these two bands to the $1b_1$ and $8a_1$ orbitals as shown in Figure 1. The $1b_1(n_{\perp})$ orbital is mostly due to the fluorine $2p_y$ orbital distributed perpendicular to the benzene ring and protrudes outside the molecular plane (Figure 5). On the other hand, the $8a_1$ orbital has fluorine $2p_z$ character and extends far outside of the C–F bond (Figure 5). Therefore, these two orbitals are expected to interact easily with metastable atoms and give strong bands in the PIES. The enhancement of the PIES band due to a C–F bonding orbital such as the $8a_1$ is also observed in the case of the $5a_1$ band in CH_3F.[27]

Bands 7 to 10 are assigned as shown in Table I on the basis of the calculated IP's. Among them, the position of the $9a_1$ band would not been found without the observation of the PIES. The $7b_2$ orbital has largely fluorine $2p_x$ character and gives a rather weak band as in the case of the $9b_2$ orbital.

To make the above argument more quantitative, we show in Figure 7 the electron density maps of the $3b_1(\pi_3)$, $2b_1(\pi_1)$, $11a_1$, $10a_1$, $1b_1(n_{\perp})$, $9a_1$, and $8a_1$ orbitals drawn on the symmetry plane perpendicular to the molecular plane. The thick curves in the maps indicate the repulsive molecular surface estimated from the van der Waals radii of the atoms (r_H = 1.20 Å, r_C = 1.70 Å, r_F = 1.35 Å). As is seen in Figure 7, the $3b_1(\pi_3)$, $2b_1(\pi_1)$, and $1b_1(n_{\perp})$ orbitals giving strong bands in PIES are widely distributed outside the molecular plane compared to the $11a_1$, $10a_1$, and $9a_1$ orbitals showing weak bands. The strong activity in PIES of the $8a_1$ orbital having fluorine $2p_z$ character is due to extension of this orbital outside and along the C–F bond, where the extension may not be well expressed by the basis set (4-31G) employed in our calculation.

(2) Chlorobenzene. In Figure 2 bands 1 to 4 and 7 are enhanced in the 11–6-eV region of the PIES. We assigned these bands to the $4b_1(\pi_3)$, $1a_2(\pi_2)$, $9b_2(n_{\parallel})$, $3b_1(n_{\perp})$, and $2b_1(\pi_1)$ orbitals. Since

(27) Fujisawa, S.; Ohno, K.; Harada, Y., to be submitted for publication.

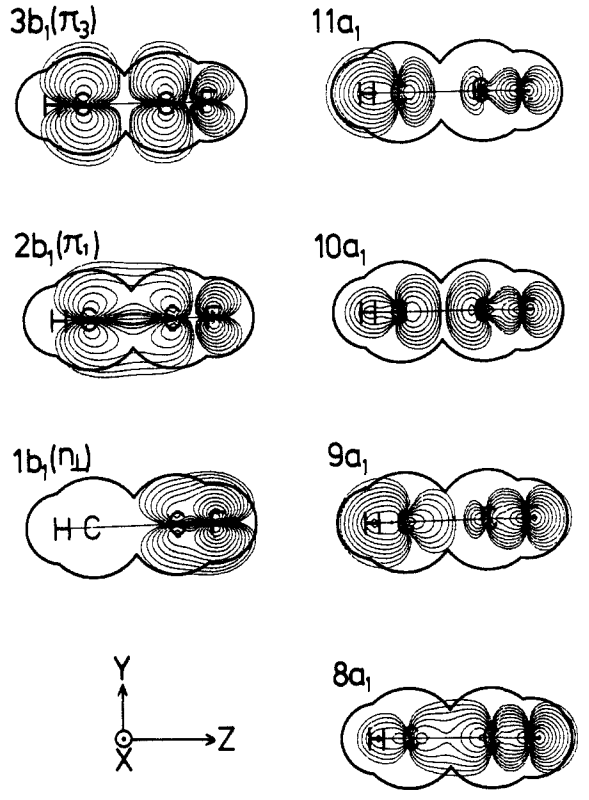

Figure 7. Electron density maps of the $3b_1(\pi_3)$, $2b_1(\pi_1)$, $11a_1$, $10a_1$, $1b_1(n_\perp)$, $9a_1$, and $8a_1$ orbitals of C_6H_5F drawn on the symmetry plane perpendicular to the molecular plane. The density of the nth line from the outside (d_n) is $2^n \times 10^{-4}$ au.

bands 3 and 4 are very sharp in the UPS, it is natural to assign them to the n orbitals. The enhancement of the bands due to the π orbitals extending outside the molecule was also seen in C_6H_5F. Furthermore, the n bands should be enhanced in C_6H_5Cl, because the n orbitals having chlorine 3p character are widely distributed outside the molecular surface. This effect of the chlorine 3p orbital is evident from the fact that even the $n_\parallel$ orbital is not effectively shielded by the benzene ring and gives a strong band in the PIES in contrast to the case of C_6H_5F showing a weak $n_\parallel$ band.

After the assignments of the π and n bands, we can easily relate bands 5 and 6 to the $15a_1$ and $8b_2$ orbitals from the comparison of the observed and calculated IP's in Table II. These orbitals are correlated to the degenerate $3e_{2g}(\sigma)$ orbital (IP 11.53 eV) of benzene. The above assignments in the IP region 9–14 eV of the UPS agree with the recent assignments by other workers.[18,19,21]

In the 14–18-eV region of the UPS, band 8–12 are assigned as shown in Table II, in which the ordering of the calculated IP's is reversed for the bands 10 and 11. This assignment is based on the following reason. Although band 10 appears strongly in the UPS, it is scarcely observed in the PIES. This can be interpreted, if band 10 is related to the $6b_2$ orbital which is localized along the C–C bonds (cf. Figure 6) and shielded by other orbitals. The electron distribution of the $6b_2$ orbital is almost the same as that of the benzene $1b_{2u}$ orbital, which also gives a very weak band in the PIES.[3,11] On the other hand, band 11 appearing clearly in the PIES can be assigned to the $13a_1$ orbital, which has hydrogen 1s and chlorine 2s and 2p character (Figure 6), and is distributed outside the molecule.

In Figure 2 the strong intensity of the $14a_1$ band in the PIES is also clear, because the $14a_1$ orbital, having the sp-hybridized character of the chlorine atom, extends far outside the molecular surface along the C–Cl bond (Figure 6). Further, the similarity of shape between band 12 in the UPS and the $3a_{1g}$ band in benzene suggests that band 12 is due to the $12a_1$ orbital correlated to the $3a_{1g}$ orbital of benzene. In the PIES in Figure 2 this band has rather large intensity. This reflects the similarity of electron distribution between the $12a_1$ orbital and the $3a_{1g}$ benzene orbital which has CH bonding character and gives a rather strong band

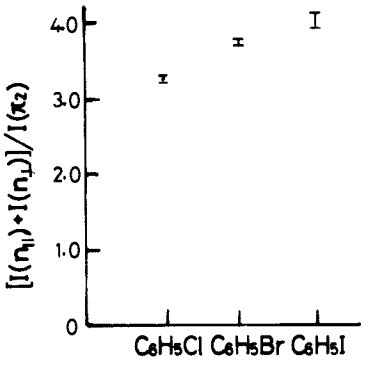

Figure 8. The relative PIES intensity of the $n_\parallel$ and $n_\perp$ bands with respect to the π_2, $[I(n_\parallel) + I(n_\perp)]/I(\pi_2)$, for C_6H_5Cl, C_6H_5Br, and C_6H_5I.

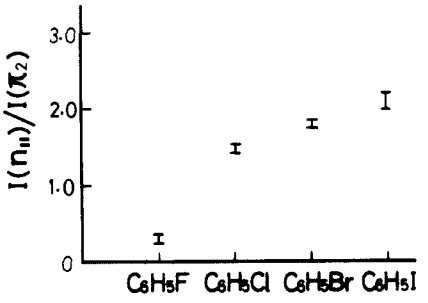

Figure 9. The relative PIES intensity of the $n_\parallel$ band with respect to the π_2, $I(n_\parallel)/I(\pi_2)$, for C_6H_5Cl, C_6H_5Br, and C_6H_5I.

in the PIES.[3] Sell et al. assigned bands 10 and 12 to the $6b_2$ and $12a_1$ orbitals, respectively, on the basis of measurements of angular distributions of the UPS.[17] Their assignments are in agreement with ours. Further, the ordering of the orbitals in Table II is the same as that proposed by Ruščić et al.[19]

(3) Bromobenzene and Iodobenzene. In Figures 3 and 4, the position of band 7 in the UPS of C_6H_5Br or C_6H_5I has been determined from the comparison of the PIES and UPS. The assignments of the observed bands in the spectra of C_6H_5Br and C_6H_5I are carried out as in the case of C_6H_5Cl and indicated in Figures 3 and 4. As before, the π and n bands are enhanced in the PIES. The change in the degrees of the enhancement on going from C_6H_5Cl to C_6H_5I will be discussed in the next section. In Tables II–IV, the orderings of the orbital type for C_6H_5Br and C_6H_5I are the same as that for C_6H_5Cl except for the bands 10 and 11. In contrast to the case of C_6H_5Cl, band 10 is stronger than band 11 in the PIES of C_6H_5Br or C_6H_5I. Therefore, in C_6H_5Br or C_6H_5I, band 10 is assigned to the a_1 orbital having the characteristics of the hydrogen and halogen orbitals, and band 11 to the b_2 orbital localized along the C–C bonds.

Our assignments of bands 1 to 7 for C_6H_5Br and C_6H_5I agree with those by Potts et al.[18] and Niessen et al.,[21] although they took wrong positions (IP = 12.27 and 12.70 eV) for the $b_2(\sigma)$ and $b_1(\pi_1)$ bands for C_6H_5Br.

Relative Reactivity of Orbitals with Metastable Atoms. In this section, we will discuss the relative reactivity of the π and n orbitals of monohalogenobenzenes upon electrophilic attack by metastable helium atoms on the basis of the relative (integrated) intensities of the π and n bands in the PIES. Since C_6H_5Cl, C_6H_5Br, and C_6H_5I have similar electronic structures, the orbital reactivities are considered mainly among them, although that of C_6H_5F is referred to occasionally. The relative band intensities of each compound were obtained with respect to the intensity of the π_2 band as a reference, because the π_2 orbital does not mix with the other orbitals owing to difference in symmetry, and also it is not shielded effectively by other orbitals from the attack of metastable atoms.

(1) Reactivity of n Orbitals. Figure 8 shows the relative intensity of the $n_\parallel$ and $n_\perp$ bands with respect to the π_2 bands, $I(n_\parallel) + I(n_\perp)/I(\pi_2)$, for C_6H_5Cl, C_6H_5Br, and C_6H_5I. As can be seen from the figure (the average relative values for the $n_\parallel$ and $n_\perp$ orbitals being 1.6–2.0), the reactivities of the n orbitals are much

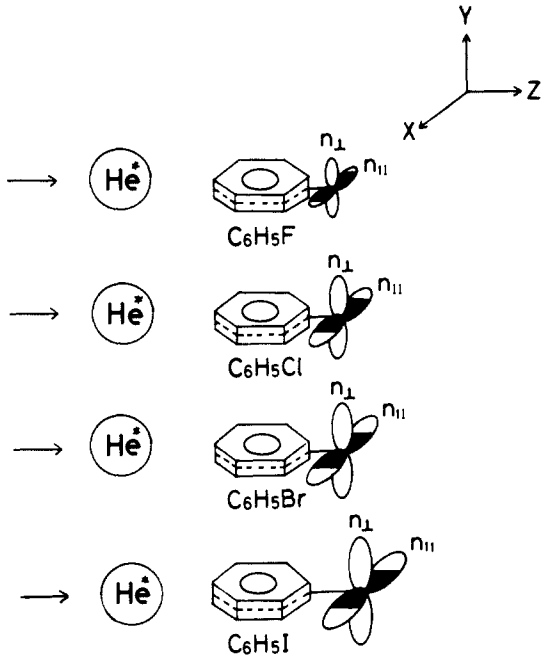

Figure 10. Schematic diagram showing the $n_\parallel$ orbital shielded by the benzene ring from the attack of a metastable atom. The shielding effect is the strongest for C_6H_5F and becomes weaker for larger n orbitals.

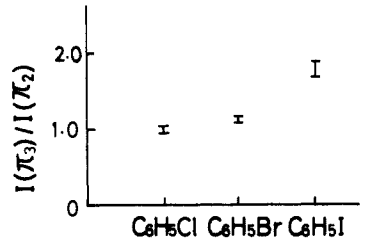

Figure 11. The relative PIES intensity of the π_3 band with respect to the π_2, $I(\pi_3)/I(\pi_2)$, for C_6H_5Cl, C_6H_5Br, and C_6H_5I.

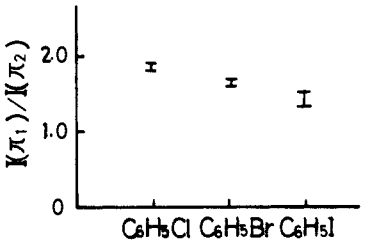

Figure 12. The relative PIES intensity of the π_1 band with respect to the π_2, $I(\pi_1)/I(\pi_2)$, for C_6H_5Cl, C_6H_5Br, and C_6H_5I.

larger than that of the π_2. This is because the n orbitals, mainly due to the halogen np orbitals (n = 3, 4, 5), extend further outside the molecule than the π_2 orbital due to the carbon 2p orbitals. The increase in the relative intensity on going from C_6H_5Cl to C_6H_5I (Figure 8) reflects the enlargement of the distribution of the halogen np orbitals.

It is a little puzzling here that the $n_\perp$ band is much enhanced relative to the π_2 band in the PIES of C_6H_5F (Figure 1), although the fluorine 2p orbital is contracted compared to the carbon 2p orbital. This may be due to the localized character of the $n_\perp$ orbital of C_6H_5F; in contrast to the case of the other monohalogenobenzenes, the $n_\perp$ orbital of C_6H_5F is originated almost purely from the fluorine 2p orbital having large electronegativity (cf. Figure 5) and hence protrude far outside the molecular surface.

Figure 9 shows the relative intensity of the $n_\parallel$ band, $I(n_\parallel)/I(\pi_2)$, for C_6H_5F, C_6H_5Cl, C_6H_5Br, and C_6H_5I. As was described before, the $n_\parallel$ orbitals are shielded by the benzene ring from the attack of metastables. This shielding effect is very strong for C_6H_5F having the contracted n orbitals and becomes much weaker for larger n orbitals, as illustratd in figure 10, which explains the change in the reactivity of the $n_\parallel$ orbitals shown in Figure 9.

(2) Reactivity of π Orbitals. Figures 11 and 12 show the relative intensities of the π_3 and π_1 bands with respect to the π_2, $I(\pi_3)/I(\pi_2)$ and $I(\pi_1)/I(\pi_2)$, for C_6H_5Cl, C_6H_5Br, and C_6H_5I. We can find from the figures that the reactivity of the π_3 orbital increases and that of the π_1 decreases from C_6H_5Cl to C_6H_5I. As will be described below, these changes can be interpreted in terms of the changes in the distributions of the π_3 and π_1 orbitals on going from C_6H_5Cl to C_6H_5I.

Figure 13 shows a correlation diagram for the π and n orbitals of C_6H_5Cl, C_6H_5Br, and C_6H_5I. As shown on the left of the figure, the π_3 and π_1 orbitals of the benzene ring interact with the halogen p_y orbital, and the degeneracies of the π (π_3 and π_2) and the p (p_x and p_y) orbitals are lifted. The ring π_3 orbital interacts with the p_y orbital more strongly, as the energy difference between them, δ_1, is smaller. Similarly, the degree of the interaction between the p_y and the π_1 ring orbitals is determined by their energy difference, δ_2. On the right of Figure 13, δ_1 is approximated to be the difference in the observed IP between the $n_\parallel$ and π_2 orbitals and δ_2 to be that between the ring π_1 and $n_\parallel$ orbitals. The position of the ring π_1 orbital (π_1 orbital before conjugation) can be estimated on the assumption that the energy separation between the ring π_1 and the π_2 orbitals is 2.86 eV,[26] the difference in IP between the $1a_{2u}(\pi)$ and $1e_{1g}(\pi)$ orbitals of benzene. In Figure 13 the δ_1 value becomes smaller, and hence the halogen p_y character for the π_3 orbital stronger on going from C_6H_5Cl to C_6H_5I. This explains the increase in the relative intensity of the π_3 band (Figure 11), because the reactivity of the π_3 orbital upon metastables increases with the increase in the character of the halogen p_y orbital having large distribution outside the molecule. It is worth noting that a marked change in δ_1 from C_6H_5Br to C_6H_5I is related to an abrupt change in the relative reactivity (Figure 11).

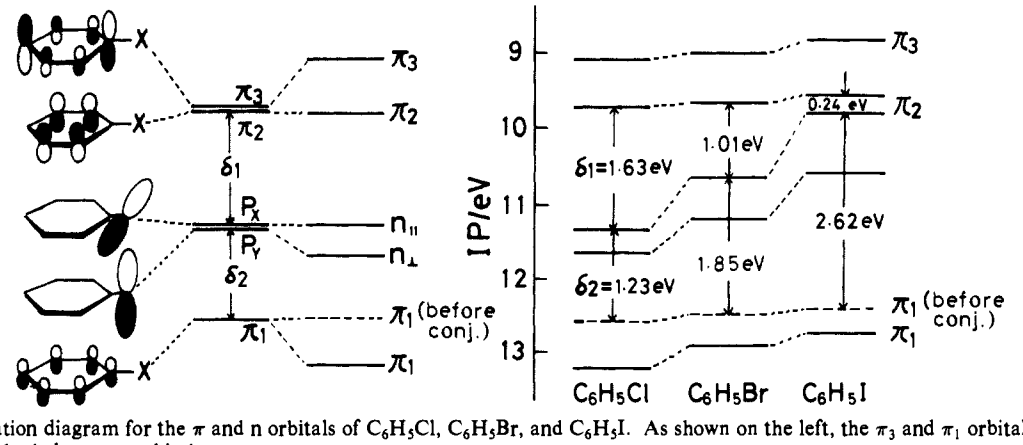

Figure 13. Correlation diagram for the π and n orbitals of C_6H_5Cl, C_6H_5Br, and C_6H_5I. As shown on the left, the π_3 and π_1 orbitals of the benzene ring interact with the halogen p_y orbital.

In Figure 13 the δ_2 value increases from C_6H_5Cl to C_6H_5I, which corresponds to the decrease in the halogen p_y character for the π_1 orbital. The fact that the relative intensity of the π_1 band in Figure 13 decreases from C_6H_5Cl to C_6H_5I despite the increase in the size of the p_y orbital shows that the effect of the p_y mixing is stronger than that of the size of the p_y orbital on the reactivity of the π_1 orbitals.

Conclusions

Penning ionization electron spectroscopy (PIES) provides direct information on the spatial distribution of individual molecular orbitals. On the basis of this unique feature of PIES, all the bands in the He I spectra of monohalogenobenzenes, C_6H_5F, C_6H_5Cl, C_6H_5Br, and C_6H_5I, have been assigned. Since Penning ionization can be interpreted as an electrophilic reaction in which an electron in an occupied orbital is extracted into the vacant orbital of the metastable atom, the relative reactivity of electrons in a particular orbital upon electrophilic attacks can be probed by PIES. By the use of this character of PIES, the relative reactivities of the n and π orbitals of monohalogenobenzenes have been studied. It is found that the orbital reactivity depends on the electronic factor due to the size of the halogen p orbitals and the conjugation between the benzene ring and the halogen atoms, and also on the steric factor due to the benzene ring shielding some orbitals from the impact of metastable atoms. Although we have selected a series of halogenobenzenes as an example, the present results are of general importance and demonstrate that PIES is a powerful technique for studying the stereochemical property and the reactivity of individual molecular orbitals.

Acknowledgment. We thank Mr. H. Mutoh and Mr. K. Imai for their help in the experiments and Mr. Y. Itoh for his help in the calculations.

Registry No. C_6H_5F, 462-06-6; C_6H_5Cl, 108-90-7; C_6H_5Br, 108-86-1; C_6H_5I, 591-50-4.

Application of Marcus Theory to Photochemical Proton-Transfer Reactions. 1. An Exploratory Study of Empirical Modifications of the Basic Equations

Keith Yates

Contribution from the Department of Chemistry, University of Toronto, Toronto, Ontario, Canada M5S 1A1. *Received December 12, 1985*

Abstract: Marcus theory has been applied empirically to photochemical proton-transfer reactions by the inclusion of an asymmetry parameter ϵ or ϵ' which is allowed to vary between 0 and 1, to reflect the fact that excited-state potential energy wells will generally be shallower than analogous ground-state surfaces. It is found that experimentally observed Brønsted α values and the curvature of the Brønsted plots can only be reasonably explained by using ϵ' values in the neighborhood of 0.3. Such values give reasonable estimates of the "intrinsic" barrier for proton transfer and probable $\Delta G°$ ranges for these reactions. Various forms of modified Marcus equations, and their relationship to intersecting parabolas of different curvature, are discussed.

Marcus theory, which was originally developed to interpret the rates of electron-transfer reactions,[1] has also been successfully applied to proton-transfer reactions.[2] It has apparently not yet been applied to any photochemical proton-transfer reactions, although there is no reason in principle why it should not be, at least for simple proton transfers involving singlet excited states. We have recently[3] reported the first examples of general acid catalysis in photochemical reactions, and the values of the Brønsted α found for these reactions, as well as the observed curvature in the Brønsted plots, can be used to test the applicability of the Marcus equations.

The theory[4] relates the free energy of activation $\Delta G^‡$ to the standard free energy of the overall reaction $\Delta G°$ via the equation:

$$\Delta G^‡ = w^r + \lambda(1 + \Delta G°/\lambda)^2/4$$
$$= w^r + \lambda/4 + \Delta G°/2 + (\Delta G°)^2/4\lambda \quad (1)$$

where w^r is the work required for solvent reorganization to form the encounter complex between substrate and catalyst, $\Delta G°$ is the actual free-energy change in the proton-transfer step itself, and $\lambda/4$ is the "intrinsic" barrier to reaction, for the case in a reaction series where $\Delta G° = 0$. Thus $\Delta G^‡$ and $\Delta G°$ are connected for a reaction series which shares a common intrinsic barrier.

Since the Brønsted α coefficient is defined as $d\Delta G^‡/d\Delta G°$, then as pointed out previously,[1,5] differentiation of (1) gives the equation:

$$d\Delta G^‡/d\Delta G° = \tfrac{1}{2} + \Delta G°/2\lambda = \alpha \quad (2)$$

The extent of curvature in a Brønsted plot can be obtained by differentiating eq 2 to give eq 3. Therefore, any observed curvature will depend on the magnitude of the intrinsic barrier for the reaction series. Slow reactions with large intrinsic barrier should show essentially linear Brønsted plots (especially over the short catalyst pK ranges normally employed), while fast reactions such as photochemical proton transfers, with low values of $\lambda/4$, should yield distinct curvature. Rates of proton transfer (k_{HA}) have been previously reported[6] for the photohydration of substituted styrenes and phenylacetylenes. Independent measurements of k_{HA} based on the pH dependences of fluorescence quenching, singlet-state lifetimes, and observed quantum yields for overall reaction gave consistent results, with k_{HA} values for these substrates being in the 1.0×10^6 to 5×10^7 M^{-1} s^{-1} range. Values of k_{HA}

$$d\alpha/d\Delta G° = 1/2\lambda \quad (3)$$

(1) Marcus, R. A. *J. Phys. Chem.* **1968**, *72*, 891; *J. Am. Chem. Soc.* **1969**, *91*, 7224.
(2) See, for example, several excellent reviews: Kresge, A. J. *Chem. Soc. Rev.* **1973**, *2*, 475; *Acc. Chem. Res.* **1975**, *8*, 354. More O'Ferrall, R. A. In *Proton Transfer Reactions* Caldin E. F., Gold, V., Eds.; Chapman and Hall: London, 1975.
(3) Wan, P.; Yates, K. *J. Org. Chem.* **1983**, *48*, 869.
(4) This presentation of Marcus theory follows the discussion of: Pross, A. *Adv. Phys. Org. Chem.* **1977**, *14*, 69.
(5) Albery, W. J.; Campbell-Crawford, A. N.; Curran, J. S. *J. Chem. Soc., Perkin Trans. 2* **1972**, 2206.
(6) Wan, P.; Culshaw, S. C.; Yates, K. *J. Am. Chem. Soc.* **1982**, *104*, 2509.

0002-7863/86/1508-6511$01.50/0